EPJ Web of Conferences **111**, 05004 (2016)
DOI: 10.1051/epjconf/201611105004

Evaluating the ^{239}Pu Prompt Fission Neutron Spectrum Induced by Thermal to 30 MeV Neutrons

D. Neudecker[1,a], P. Talou[1], T. Kawano[1], A.C. Kahler[1], M.E. Rising[1], and M.C. White[1]

[1] *Los Alamos National Laboratory, P.O. Box 1663, Los Alamos, NM 87545, USA*

Abstract. We present a new evaluation of the ^{239}Pu prompt fission neutron spectrum (PFNS) induced by thermal to 30 MeV neutrons. Compared to the ENDF/B-VII.1 evaluation, this one includes recently published experimental data as well as an improved and extended model description to predict PFNS. For instance, the pre-equilibrium neutron emission component to the PFNS is considered and the incident energy dependence of model parameters is parametrized more realistically. Experimental and model parameter uncertainties and covariances are estimated in detail. Also, evaluated covariances are provided between all PFNS at different incident neutron energies. Selected evaluation results and first benchmark calculations using this evaluation are briefly discussed.

1 Introduction

A prompt fission neutron spectrum (PFNS) provides the energy distribution of neutrons emitted promptly after fission and before the onset of delayed β-decay. The PFNS of ^{239}Pu is a quantity of high interest for nuclear data applications including reactor physics and global security. For instance, a reliably evaluated ^{239}Pu PFNS is key to accurately simulate the reactivity of chain reactions in a nuclear reactor. Therefore, significant efforts have been undertaken to provide improved evaluated nuclear data within the framework of an IAEA coordinated research project on PFNS of actinides [1] as well as for the CIELO project [2] and the next release of the ENDF/B-library.

Here, we present a new evaluation of the ^{239}Pu PFNS induced by neutrons with incident energies from thermal to 30 MeV. This evaluation is currently tested as part of a CIELO prototype file for incident energies above 5 MeV and was also distributed to the IAEA CRP [1]. Compared to the ENDF/B-VII.1 evaluation [3], improved experiment and model inputs were included in the evaluation as described in Section 2. Changes compared to ENDF/B-VII.1 are discussed in Section 3, along with first benchmark results. Section 4 offers a brief summary and an outlook for future work.

2 Evaluation methodology and input

Evaluated data ψ and covariances Cov^{ψ} are provided for incident neutron energies E_{inc} = {thermal, 0.5, 1, 2, 3, 4, 5, 5.5, 6, 6.5, 7, 8, 9, 10, 11, 11.5, 12, 13, 14, 15, 17.5, 20, 30} MeV and for each

[a] e-mail: dneudecker@lanl.gov

Table 1. The first author, main references, incident energies, outgoing energy range and range of relative uncertainties are given for the experimental database included in the evaluation.

Author	References	E_{inc}	E_{out} (MeV)	Rel. Unc. (%)
Starostov combined	[4–7]	thermal	0.025–11.3	2–73
Lajtai et al.	[8]	thermal	0.025–4.0	9–47
Knitter	[9]	0.215 MeV	0.28–13.87	4–347
Lestone et al.	[10]	1.5 MeV	1.5–11.5	2–112
Chatillon et al.	[11, 12]	1-15 MeV	0.3–8.25	5–120

E_{inc} for the same outgoing energy grid E from 10^{-5} to 30 MeV. They were obtained by the frequently employed generalized least squares algorithm:

$$\psi = N + \text{Cov}^{\psi} S^t (\text{Cov}^{\phi})^{-1} (\phi - SN) \text{ and } \text{Cov}^{\psi} = \text{Cov}^{N} - \text{Cov}^{N} S^t \left(S \, \text{Cov}^{N} S^t + \text{Cov}^{\phi} \right)^{-1} S \, \text{Cov}^{N}. \quad (1)$$

The variables N and ϕ denote model predicted PFNS values and experimental data and Cov^{N} and Cov^{ϕ} their respective covariances. The design matrix S and its transpose S^t are calculated by linear interpolation taking into account E_{inc} and the outgoing neutron energy E of N and ϕ.

Experimental input

The experimental data ϕ included in the evaluation through Eq. (1) are listed in Table 1. The data of Lestone et al. [10] and Chatillon et al. [11] were recently published and are thus not included in the ENDF/B-VII.1 evaluation. The latter data were corrected following the work of Granier [12]. We did not include Chatillon et al. data for $E_{\text{inc}} > 15$ MeV as the measurement does not capture the full pre-equilibrium component of the PFNS contrary to our model values. If we include the data for $E_{\text{inc}} > 15$ MeV, this physics discrepancy between model and experiment will lead to biased evaluated data. The data of [4–7] were statistically combined into one data set, which we term here "Starostov combined".

The experimental covariances Cov^{ϕ} appearing in Eq. (1) were estimated in great detail for each data set and covariances between different data sets were estimated as well [13]. The total uncertainties given in Table 1 are for most experiments larger than those found in their respective EXFOR entries. The uncertainties had to be increased after recent Monte Carlo transport studies [12–14] of the experimental set-ups of [4–9, 11] indicated possible biases of the experimental data due to e.g., multiple scattering. These effects were not considered for the evaluation of ENDF/B-VII.1. The experimental data and covariances for this evaluation will be published at https://www-nds.iaea.org/pfns/.

Model input

The model values N and covariances Cov^{N} were calculated using the code CoH [15]. It gives N in the laboratory frame with outgoing neutron energy E by

$$N(E) = \Big\{ \nu_1 N_1(E) P_{f1} + [\chi_1(E) + \nu_2 N_2(E)] P_{f2} + [\chi_1(E) + \chi_2(E) + \nu_3 N_3(E)] P_{f3} \quad (2)$$
$$+ [\chi_1(E) + \chi_2(E) + \chi_3(E) + \nu_4 N_4(E)] P_{f4} \Big\} / \Big\{ \nu_1 P_{f1} + [1 + \nu_2] P_{f2} + [2 + \nu_3] P_{f3} + [3 + \nu_4] P_{f4} \Big\}.$$

The spectra $\chi_i(E)$ describe the emission of $i = \{1, 2, 3\}$ neutron(s) prior to fission. These pre-fission neutrons are emitted in pre-equilibrium and compound processes, and result in a pre-fission neutron spectrum which is added to the PFNS. Only neutrons are considered that lead to a residual nucleus

with enough energy to fission. The pre-equilibrium component was not considered in ENDF/B-VII.1. The variables $N_i(E)$ are the spectra of neutrons emitted promptly after fission in first-chance ($i = 1$), second-chance ($i = 2$), etc., processes and are calculated by an extended version [16] of the Los Alamos model [17] (LAM), while the exciton model was used for the pre-equilibrium component. The variables P_{fi} yield the probability that fission of i^{th} chance occurs. The fission barrier parameters used to calculate P_{fi} were fitted to reproduce P_{fi} from ENDF/B-VII.0. N_i are weighted with ν_i, the average number of neutrons emitted.

The total kinetic energy carried away by the fission fragments and the energy release are important parameters of the LAM and are known—from measurements and theoretical considerations—to depend on E_{inc}. This E_{inc}-dependence was considered following Refs. [18, 19], while the total kinetic energy was assumed to be constant for the ENDF/B-VII.1 evaluation. Also, uncertainties of more model parameters following [16] were included for this evaluation compared to ENDF/B-VII.1.

3 Results and discussion

Evaluated data ψ and covariances $\mathbf{Cov}^{\psi}$ are obtained by Eq. (1) and the experimental and model inputs of Section 2. The experimental data set Starostov combined [4–7] and Lestone et al. [10] have the highest precision of our experimental database. The evaluated results presented here (termed "Current") at E_{inc} = thermal and 1.5 MeV follow both data sets closely as shown in the upper panels of Fig. 1. The ENDF/B-VII.1 evaluation [3] also follows the data of Lestone et al. closely at E_{inc} = 1.5 MeV. For E_{inc} = thermal, ENDF/B-VII.1 has a trend to lower PFNS values for $E_{\text{out}} \leq 0.8$ MeV compared to the combined Starostov data as well as the current evaluation.

The shapes of ENDF/B-VII.1 and the current evaluation differ distinctly for $E_{\text{inc}} = 6$ and 14 MeV in the lower panels of Fig. 1 due to the improvements made in the model description. In ENDF/B-VII.1, all neutrons evaporated from the initial and subsequent compound nuclei are counted, while in the current evaluation only those neutrons associated with the fission process are considered. This difference results in the bump at 300 keV in the current evaluation for $E_{\text{inc}} = 6$ MeV. This bump stems from the superposition of first and second chance fission contributions to the PFNS, where the latter drops off sharply at a threshold defined by the energy needed to overcome the fission barrier. At $E_{\text{inc}} =$ 14 MeV, the difference in the shape (e.g., the peak around $E = 8$ MeV) arises from the pre-equilibrium component, which was not considered for ENDF/B-VII.1. For $E_{\text{inc}} > 1.5$ MeV, only the data Chatillon et al. [11] were deemed accurate and precise enough to be included in the evaluation. However, they do not conclusively support one evaluation over the other. The Chi-Nu project at LANSCE [20], which aims at delivering ^{239}Pu PFNS precision data for $E_{\text{inc}} = 0.5$–20 MeV, might provide more conclusive answers in the near future.

First benchmarks results are presented in Table 2 for the criticality k_{eff} of the Jezebel (PMF1), Flattop-Pu (PMF6) and a suite of thermal solution (PST) assemblies [21]. They were frist calculated using ENDF/B-VII.1 data, and then with a modified ENDF/B-VII.1 file, which was updated with the current evaluation, the findings of the WPEC SG34 [22] on the neutron multiplicity and CIELO ^{16}O data [2]. Jezebel and Flattop benchmarks are higher than 1 for ENDF/B-VII.1 and are now lower. The k_{eff} values for the suite of seven PSTs is slightly closer to 1 than the respective ENDF/B-VII.1 value, mostly due to new ^{16}O data. While these results look encouraging, one has to consider that a critical assembly benchmark is not a *sufficient* validation constraint of evaluated data, as many reactions contribute to calculations of assemblies and biases in several of them might compensate each other.

Evaluated covariances Cov^{ψ} are also provided as part of the same evaluation and for each incident energy as well as between different incident energies. In Ref. [23], it is shown that neglecting those cross-correlations between different incident energies results in an under-prediction of the k_{eff} uncertainty caused by the ^{239}Pu PFNS of Jezebel and Flattop by up to 50%.

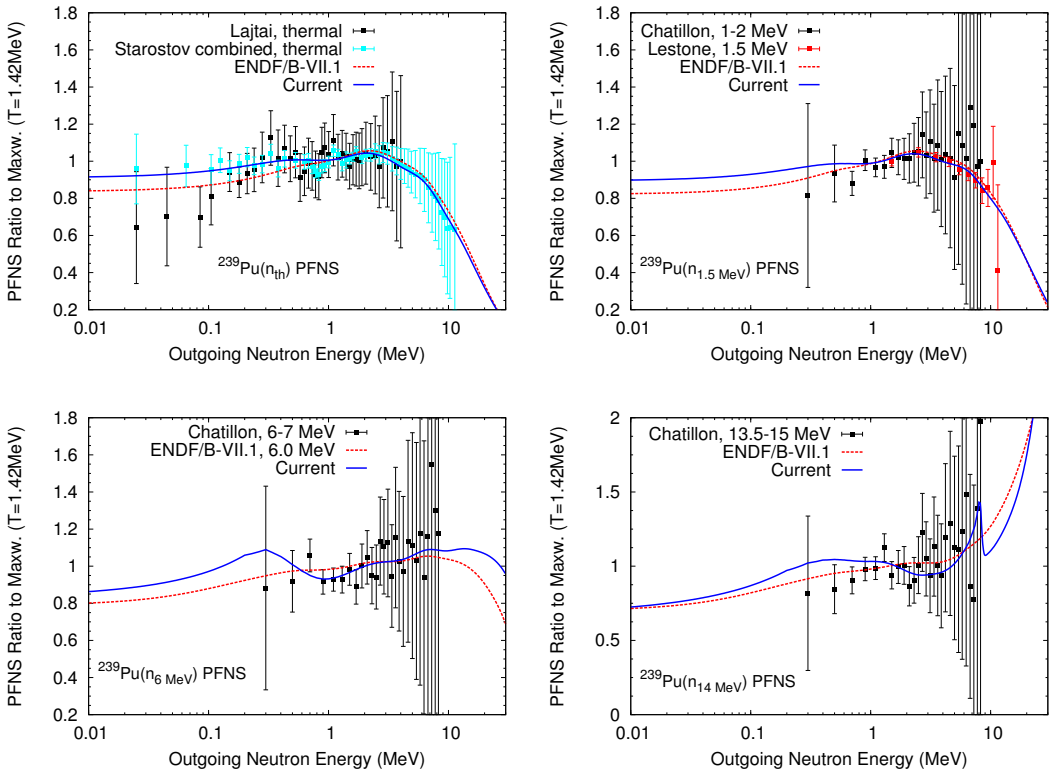

Figure 1. The evaluated data for E_{inc} = thermal, 1.5, 6 and 14 MeV ("Current") are compared to the ENDF/B-VII.1 evaluation and experimental data of the same E_{inc} (scaled to the current evaluation). The current evaluated data at E_{inc} = 1.5 MeV were obtained by averaging evaluated data at 1 and 2 MeV in order to compare to the data of Lestone et al.

Table 2. Benchmark calculations of k_{eff} for Jezebel (PMF1), Flattop-Pu (PMF6) and an average of a suite of seven thermal solution assemblies (PST) is shown using ENDF/B-VII.1 and the current evaluation. The suite of PSTs comprises PST1.4, PST4.1, PST12.10, PST12.13, PST18.6, PST34.4 and PST 34.15. The naming convention follows the ICSBEP handbook [21].

Evaluation	PMF1	PMF6	PST averages
ENDF/B-VII.1	1.00061	1.00111	1.00388
Current	0.99908	0.99946	1.00295

4 Summary and outlook

We presented an evaluation of the ^{239}Pu prompt fission neutron spectrum (PFNS) for incident neutron energies from thermal to 30 MeV, which was submitted to the IAEA Coordinated Research Project on PFNS [1] and is partially implemented in a CIELO test file [2]. Compared to the ENDF/B-VII.1 evaluation [3], (1) recently published experimental data [10, 11] were implemented, (2) detailed experimental uncertainties were estimated including uncertainties associated with previously unknown possible biases [13, 14], (3) the original Los Alamos model [17] was extended [16], (4) the pre-equilibrium

component to the PFNS was considered and (5) the incident energy dependence of important model parameters was included in the model description following [18, 19]. The evaluated results shown in Fig. 1 follow high precision experimental data and differ in shape—especially above the second chance fission threshold—from the ENDF/B-VII.1 evaluation. Initial criticality benchmarks show small but acceptable changes compared to ENDF/B-VII.1.

Benchmarking is ongoing, partially within the CIELO project, to study also the effect of compensating errors in other reactions and isotopes. Finally, an incident energy dependent evaluation of the ^{235}U PFNS along the same lines is in progress.

Acknowledgements

We would like to acknowledge the valuable input of R. Capote, M.B. Chadwick, J.J. Egan, Th. Granier, R.C. Haight, H.Y. Lee, J.P. Lestone, W. Mannhart, J.M. O'Donnell, N. Otsuka, V. Pronyaev, A. Sardet, T.N. Taddeucci, D.L. Smith, P. Staples and J. Taieb. This work at LANL was sponsored by the NNSA, US DoE under Contract No. DE-AC52-06NA25396.

References

[1] R. Capote et al., Nuclear Data Sheets, submitted (2016)
[2] M.B. Chadwick et al., Nuclear Data Sheets **118**, 1 (2014)
[3] M.B. Chadwick et al., Nuclear Data Sheets **112**, 2887 (2011)
[4] V.N. Nefedov et al., IAEA Vienna Report INDC(CCP)-0457 (2014), EXFOR-No. 40871
[5] A.A. Boytsov et al., IAEA Vienna Report INDC(CCP)-0459 (2014), EXFOR-No. 40873
[6] B.I. Starostov et al., IAEA Vienna Report INDC(CCP)-0458 (2014), EXFOR-No. 40872
[7] B.I. Starostov et al., IAEA Vienna Report INDC(CCP)-293/L, 19 (1989), EXFOR-No. 40930
[8] A. Lajtai et al., Proceedings of the Conf. on Nuclear Data for Basic and Applied Sciences, Santa Fe 1985 **1**, 613 (1985), EXFOR-No. 30704
[9] H.-H. Knitter, Atomkernenergie **26**, 76 (1975), EXFOR-No. 20576
[10] J.P. Lestone et al., Nuclear Data Sheets **119**, 213 (2014)
[11] A. Chatillon et al., Physical Review C **89**, 014611 (2014)
[12] Th. Granier, Phys. Procedia **64**, 183 (2015)
[13] D. Neudecker et al., Nuclear Data Sheets, submitted (2016); Los Alamos National Laboratory Report LA-UR-15-20824 (2015)
[14] T.N. Taddeucci et al., Nuclear Data Sheets **123**, 135 (2015)
[15] T. Kawano et al., Journal of Nuclear Science and Technology **47**, 462 (2010)
[16] D. Neudecker et al., Nuclear Instruments and Methods in Physics Research A **791**, 80 (2015)
[17] D.G. Madland and J.R. Nix, Nuclear Science Engineering **81**, 213 (1982)
[18] J.P. Lestone et al., Nuclear Data Sheets **118**, 208 (2014)
[19] D.G. Madland, Nuclear Physics A **772**, 113 (2006)
[20] R.C. Haight et al., Nuclear Data Sheet **123** (2015)
[21] *International Handbook of Evaluated Criticality Safety Benchmark Experiments* (OECD Nuclear Energy Agency Report NEA/NSC/DOC(95)03, 2013)
[22] C. de Saint Jean et al., OECD Nuclear Energy Agency Report NEA/WPEC-34 (2015)
[23] M.E. Rising et al., ICNC 2015 proceeding, submitted (2015); Los Alamos National Laboratory Report LA-UR-15-24045 (2015)